Relating small neutrino masses and mixing*

Soumita Pramanick†, Amitava Raychaudhuri‡

Department of Physics, University of Calcutta, 92 Acharya Prafulla Chandra Road, Kolkata 700009, India

Abstract

Experiments on neutrino oscillations have uncovered several small parameters, θ_{13} being a prominent one. Others are the solar mass splitting *vis-à-vis* the atmospheric one and the deviation of θ_{23} from maximal mixing. In this talk we elaborate on a neutrino mass model based on the see-saw mechanism in which the mixing angles to start with are either vanishing (θ_{13} and θ_{12}) or $\pi/4$ (θ_{23}). The atmospheric mass splitting is taken as a part of this initial structure but the solar splitting is absent. A perturbative contribution, originating from a Type-I see-saw, results in non-zero values of θ_{13}, θ_{12}, Δm^2_{solar}, and shifts θ_{23} slightly from $\pi/4$, interrelating them all. The model incorporates CP-violation, the phase δ being close to $3\pi/2$ for (a) quasi-degeneracy or (b) inverted mass ordering. It will be put to test as the neutrino parameters get better determined.

Key Words: Neutrino mixing, θ_{13}, Leptonic CP-violation, Neutrino Mass ordering, Perturbation

I Introduction

Neutrino mass and mixing have been subjects of intensive exploration as they shed light on the physics beyond the standard model. Atmospheric and solar neutrinos indicate two very different scales of neutrino mass splitting – $\Delta m^2_{solar}/|\Delta m^2_{atm}| \sim 10^{-2}$ – which are confirmed in accelerator and reactor experiments. The lepton mixing is captured in the PMNS matrix[1]. The global fits to the data [2, 3] from atmospheric, solar, accelerator, and reactor experiments indicate θ_{13} to be small [4] ($\sin\theta_{13} \sim 0.1$) and θ_{23} to be near maximal ($\sim \pi/4$). Here we discuss a model in which the atmospheric mass splitting with maximal mixing in this sector, $\theta_{23} = \pi/4$, follows from a zero-order mass matrix which sets the scale of the problem. There is at this stage no solar splitting and the other two mixing angles are also absent[2]. θ_{13} and a small shift to θ_{23} arise from a Type-I see-saw [5] contribution which also results in the solar mass splitting, acting as a perturbation. A non-zero θ_{12} is also produced and due to the degeneracy of masses it is not small. The three non-zero mixing angles open the possibility of CP-violation in the lepton sector. This model accommodates a CP-phase δ which must be close to maximal ($\delta \sim \pi/2,\ 3\pi/2$) if the neutrinos have an inverted mass ordering or if they are quasidegenerate [6]. Earlier work which partially address similar issues can be traced to [7, 8], but to our knowledge this is the first time that *all* the small parameters have been shown to have the same perturbative origin and are consistent with the latest data.

*Talk given by A. Raychaudhuri at the International Conference on Massive Neutrinos, IAS, NTU, Singapore, February 2015.

†e-mail: soumitapramanick5@gmail.com

‡e-mail: palitprof@gmail.com

[1]We use the PDG [1] parametrization of the PMNS matrix.

[2]One mixing angle being $\pi/4$ and the other two zero can be a manifestation of some underlying symmetry.

II The model

The starting choice of the mixing angles imply the following form of the mixing matrix, the columns of it being the unperturbed flavour basis[3]:

$$U^0 = \begin{pmatrix} 1 & 0 & 0 \\ 0 & \sqrt{\frac{1}{2}} & \sqrt{\frac{1}{2}} \\ 0 & -\sqrt{\frac{1}{2}} & \sqrt{\frac{1}{2}} \end{pmatrix} \quad . \tag{1}$$

Solar splitting is absent at this stage causing the first two mass eigenvalues to be degenerate[4]. Thus the unperturbed neutrino mass matrix is $M^0 = \text{diag}\{m_1^{(0)}, m_1^{(0)}, m_3^{(0)}\}$ in the mass basis. The unperturbed mass eigenvalues are made real and positive by suitable choices of the Majorana phases. The atmospheric splitting is given by $\Delta m^2_{atm} = (m_3^{(0)})^2 - (m_1^{(0)})^2$. It is useful to define $m^{\pm} = m_3^{(0)} \pm m_1^{(0)}$ and express the unperturbed mass matrix in flavour basis as,

$$(M^0)^{flavour} = U^0 M^0 U^{0T} = \frac{1}{2} \begin{pmatrix} 2m_1^{(0)} & 0 & 0 \\ 0 & m^+ & m^- \\ 0 & m^- & m^+ \end{pmatrix} \quad . \tag{2}$$

As already hinted, the perturbation can originate from a Type-I see-saw. In order to reduce the number of independent parameters the Dirac mass term is taken to be proportional to the identity, i.e., $M_D = m_D \, \mathbb{I}$, in the flavour basis. This choice completely determines the right-handed flavour basis although the form of $M_R^{flavour}$ can be chosen at will to suit our purpose. In the interest of minimality we seek symmetric matrices with the fewest non-zero entries. Five texture zero matrices fail the invertibility criterion[5] and therefore are not pursued. Next we try four texture zero options. By examining the different alternatives it can be seen that all the perturbation goals that we have set for ourselves could be achieved by only two such candidates out of which one is scripted below[6]:

$$M_R^{flavour} = m_R \begin{pmatrix} 0 & xe^{-i\phi_1} & 0 \\ xe^{-i\phi_1} & 0 & 0 \\ 0 & 0 & ye^{-i\phi_2} \end{pmatrix} \quad , \tag{3}$$

where x, y are dimensionless constants of $\mathcal{O}(1)$. The Dirac mass is kept real without any loss of generality.

III Real M_R ($\phi_1 = 0$ or $\pi, \phi_2 = 0$ or π)

For notational simplicity in this section the phases are not written explicitly, instead x (y) is taken as positive or negative depending on whether ϕ_1 (ϕ_2) is 0 or π.

Employing Type-I see-saw one can write,

$$M'^{mass} = U^{0T} \left[M_D^T (M_R^{flavour})^{-1} M_D \right] U^0 = \frac{m_D^2}{\sqrt{2}\, xym_R} \begin{pmatrix} 0 & y & y \\ y & \frac{x}{\sqrt{2}} & -\frac{x}{\sqrt{2}} \\ y & -\frac{x}{\sqrt{2}} & \frac{x}{\sqrt{2}} \end{pmatrix} \quad . \tag{4}$$

[3] In this flavour basis the charged lepton mass matrix is taken to be diagonal.

[4] Due to this degeneracy θ_{12} is arbitrary and can be chosen to be zero as done here.

[5] Existence of the inverse of M_R is an essential condition for the see-saw mechanism.

[6] The other alternative is a mere $2 \leftrightarrow 3$ exchange of this configuration and the corresponding results vary only up to a relative sign.

The changes in the solar sector are determined by the 2×2 submatrix of M'^{mass},

$$M'^{mass}_{2\times 2} = \frac{m_D^2}{\sqrt{2}\, xym_R} \begin{pmatrix} 0 & y \\ y & x/\sqrt{2} \end{pmatrix} . \tag{5}$$

From the above one has

$$\tan 2\theta_{12} = 2\sqrt{2} \left(\frac{y}{x}\right) . \tag{6}$$

The tribimaximal mixing value of θ_{12}, which is disallowed by the 1σ data but is allowed in the 3σ range[7], is obtained if $y/x = 1$. From the data, $\tan 2\theta_{12} > 0$ always, forcing x and y to have the same sign. Thus it can be inferred that either $\phi_1 = 0 = \phi_2$ or $\phi_1 = \pi = \phi_2$. The global fits of θ_{12} provide a bound on this ratio as,

$$0.682 < \frac{y}{x} < 1.075 \text{ at } 3\sigma . \tag{7}$$

From eq. (5),

$$\Delta m^2_{solar} = \frac{m_D^2}{xym_R}\, m_1^{(0)} \sqrt{x^2 + 8y^2} . \tag{8}$$

The first order corrected third wave function $|\psi_3\rangle$ is:

$$|\psi_3\rangle = \begin{pmatrix} \kappa \\ \frac{1}{\sqrt{2}}(1 - \frac{\kappa}{\sqrt{2}}\frac{x}{y}) \\ \frac{1}{\sqrt{2}}(1 + \frac{\kappa}{\sqrt{2}}\frac{x}{y}) \end{pmatrix} \quad , \tag{9}$$

where

$$\kappa \equiv \frac{m_D^2}{\sqrt{2}\, xm_R m^-} \quad . \tag{10}$$

If $x > 0$ the sign of m^- determines that of κ. Comparing eq. (9) with the third column of the PMNS matrix, we write,

$$\sin\theta_{13} \cos\delta = \kappa = \frac{m_D^2}{\sqrt{2}\, xm_R m^-} \quad , \tag{11}$$

For normal mass ordering (NO), $\delta = 0$ while for inverted mass ordering (IO) $\delta = \pi$ if $x > 0$, both being CP conserving[8]. For $x < 0$ NO (IO) corresponds to $\delta = \pi$ (0). From eqs. (11), (6), and (8) we get,

$$\Delta m^2_{solar} = \text{sgn}(x)\; m^- m_1^{(0)}\; \frac{4 \sin\theta_{13} \cos\delta}{\sin 2\theta_{12}} , \tag{12}$$

which relates the solar sector with θ_{13}. The requirement $\Delta m^2_{solar} > 0$ is ensured by $\text{sgn}(x)\; m^- \sin\theta_{13} \cos\delta > 0$ from eq. (11). If the neutrino mass splittings, θ_{12}, and θ_{13} are given, eq. (12) determines the lightest neutrino mass, m_0.

Inverted ordering is excluded by eq. (12) as we now show. If $z \equiv m^- m_1^{(0)}/\Delta m^2_{atm}$ and $m_0/\sqrt{|\Delta m^2_{atm}|} \equiv \tan\xi$, then

$$\begin{aligned} z &= \sin\xi/(1 + \sin\xi) \text{ (normal ordering)}, \\ z &= 1/(1 + \sin\xi) \text{ (inverted ordering)} . \end{aligned} \tag{13}$$

[7]From [2] we use $7.03 \leq \Delta m^2_{21}/10^{-5}\,\text{eV}^2 \leq 8.03$ and $31.30^\circ \leq \theta_{12} \leq 35.90^\circ$ at 3σ.

[8]The usual convention of all the mixing angles θ_{ij} belonging to the the first quadrant is followed.

It is seen that $0 \leq z \leq 1/2$ for NO and $1/2 \leq z \leq 1$ for IO and as $z \to 1/2$ one approaches quasidegeneracy, i.e., $m_0 \to$ large, in both cases. From eq. (12)

$$z = \left(\frac{\Delta m^2_{solar}}{|\Delta m^2_{atm}|}\right)\left(\frac{\sin 2\theta_{12}}{4\sin\theta_{13}|\cos\delta|}\right) \quad , \tag{14}$$

where $|\cos\delta| = 1$ for real M_R. For the observed ranges of the oscillation parameters $z \sim 10^{-2}$, as a result of which inverted mass ordering is disallowed.

From eq. (9):

$$\tan\theta_{23} \equiv \tan(\pi/4 - \omega) = \frac{1 - \frac{\kappa}{\sqrt{2}}\frac{x}{y}}{1 + \frac{\kappa}{\sqrt{2}}\frac{x}{y}} \quad , \tag{15}$$

Using eqs. (6) and (11) in the above we get,

$$\tan\omega = \frac{2\sin\theta_{13}\cos\delta}{\tan 2\theta_{12}} \, . \tag{16}$$

The octant of θ_{23} is dictated by the sign of ω which in its turn is determined by δ. θ_{23} lies in the first (second) octant, when ω is positive (negative), i.e., $\delta = 0$ (π). For NO, the only allowed option, this corresponds to $x > 0$ ($x < 0$).

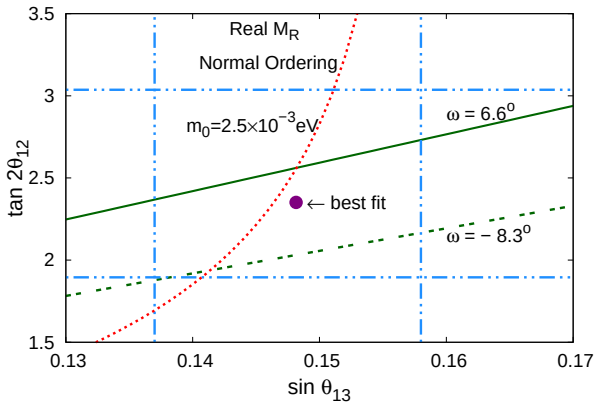

Figure 1: The 3σ range of $\sin\theta_{13}$ and $\tan 2\theta_{12}$ from global fits is represented by the blue dot-dashed box with the best-fit shown as a violet dot. When the best-fit values of the two mass-splittings are used, eq. (12) gives the red dotted curve for $m_0 = 2.5$ meV. From eq. (16) for the first (second) octant the portion below the green solid (dashed) straight line is excluded by θ_{23} at 3σ. Eq. (12) does not allow inverted ordering for real M_R.

Our results for the real perturbation are shown in Fig. 1. The 3σ global-fit range of $\sin\theta_{13}$ and $\tan 2\theta_{12}$ is marked by the blue dot-dashed box and the best-fit value is indicated by a violet dot in Fig 1. For any point in this region, if the two mass splittings are specified, the z (or equivalently m_0) that produces the correct solar splitting is determined by eq. (14).

From the 3σ data $\omega_{min} = 0$ for both octants and $\omega_{max} = 6.6^\circ$ (-8.3°) for the first (second) octant [2]. In this model in case of real M_R we get $|\omega| \geq 5.14^\circ$ for both octants using eq. (16), as $|\cos\delta| = 1$. This limits the range in which θ_{23} can be obtained[9]. Eq. (16) for ω_{max} for the first (second) octant is

[9]This range is excluded at 1σ for the first octant.

denoted by the green solid (dashed) straight lines below which the model does not hold in each case. Needless to mention that the best-fit point is allowed only if θ_{23} is in the second octant.

One obtains $z_{max} = 6.03 \times 10^{-2}$ using the 3σ limits of θ_{13} and θ_{12} in eq. (14), implying $(m_0)_{max} = 3.10$ meV. The consistency of eq. (14) with eq. (16) at ω_{max} sets $z_{min} = 4.01 \times 10^{-2}$ (3.88×10^{-2}) for the first (second) octant corresponding to $(m_0)_{min} = 2.13$ (2.06) meV. For example, if $m_0 = 2.5$ meV and if the best-fit values of the solar and atmospheric mass splittings are used then eq. (12) yields the red dotted curve in Fig. 1.

The free parameters here are m_0, m_D^2/xm_R and y for real M_R with which the solar mass splitting, $\theta_{12}, \theta_{13}, \theta_{23}$ are obtained for normal mass ordering. Inverted ordering is not allowed so long as the perturbation is real.

IV Complex M_R

For the more general complex M_R in the mass basis one gets in place of eq. (4):

$$M'^{mass} = \frac{m_D^2}{\sqrt{2}xym_R} \begin{pmatrix} 0 & ye^{i\phi_1} & ye^{i\phi_1} \\ ye^{i\phi_1} & \frac{xe^{i\phi_2}}{\sqrt{2}} & \frac{-xe^{i\phi_2}}{\sqrt{2}} \\ ye^{i\phi_1} & \frac{-xe^{i\phi_2}}{\sqrt{2}} & \frac{xe^{i\phi_2}}{\sqrt{2}} \end{pmatrix} . \tag{17}$$

Here x and y are positive. One observes that M' in eq. (17) is not hermitian. To proceed, one chooses the hermitian combination $(M^0 + M')^\dagger(M^0 + M')$ treating $M^{0\dagger}M^0$ as the zeroth order term and $(M^{0\dagger}M' + M'^\dagger M^0)$ as the lowest order perturbation. The unperturbed eigenvalues now are $(m_i^{(0)})^2$ and the perturbation matrix, which is hermitian by construction, is

$$(M^{0\dagger}M' + M'^\dagger M^0)^{mass} = \frac{m_D^2}{\sqrt{2}xym_R} \begin{pmatrix} 0 & 2m_1^{(0)}y\cos\phi_1 & yf(\phi_1) \\ 2m_1^{(0)}y\cos\phi_1 & \frac{2}{\sqrt{2}}m_1^{(0)}x\cos\phi_2 & -\frac{1}{\sqrt{2}}xf(\phi_2) \\ yf^*(\phi_1) & -\frac{1}{\sqrt{2}}xf^*(\phi_2) & \frac{2}{\sqrt{2}}m_3^{(0)}x\cos\phi_2 \end{pmatrix} , \tag{18}$$

with

$$f(\xi) = m^+\cos\xi - im^-\sin\xi \ . \tag{19}$$

Beyond this point steps similar to those for real M_R are followed.

From eq. (18) the solar mixing angle now is

$$\tan 2\theta_{12} = 2\sqrt{2}\ \frac{y}{x}\ \frac{\cos\phi_1}{\cos\phi_2} . \tag{20}$$

Thus, $(\cos\phi_1/\cos\phi_2)$ has to be positive. The limits given in eq. (7) will now apply on the combination $(y/x)(\cos\phi_1/\cos\phi_2)$.

In the complex M_R case including first order corrections $|\psi_3\rangle$ becomes

$$|\psi_3\rangle = \begin{pmatrix} \kappa f(\phi_1)/m^+ \\ \frac{1}{\sqrt{2}}(1 - \frac{\kappa}{\sqrt{2}}\frac{x}{y}\ f(\phi_2)/m^+) \\ \frac{1}{\sqrt{2}}(1 + \frac{\kappa}{\sqrt{2}}\frac{x}{y}\ f(\phi_2)/m^+) \end{pmatrix} . \tag{21}$$

Now κ is positive (negative) for NO (IO) always. Eq. (21) implies

$$\begin{aligned} \sin\theta_{13}\cos\delta &= \kappa\cos\phi_1 \ , \\ \sin\theta_{13}\sin\delta &= \kappa\ \frac{m^-}{m^+}\sin\phi_1 \quad . \end{aligned} \tag{22}$$

So, $\cos\delta$ has the same sign (opposite sign) as that of $\cos\phi_1$ for NO (IO). Further, the product $\sin\theta_{13}\sin\delta$ in the CP-violation Jarlskog parameter, J, is dependent on $\sin\phi_1$. The phase ϕ_2 has no affect on δ.

For normal ordering – $\kappa > 0$ – the quadrants of δ and ϕ_1 are the same while for inverted ordering – $\kappa < 0$ – δ has to be in the first (third) quadrant when ϕ_1 happens to be in the second (fourth) quadrant and *vice-versa*. So, a near-maximal $\delta = 3\pi/2 - \epsilon$ can be obtained if $\phi_1 \sim 3\pi/2 - \epsilon$ $(3\pi/2 + \epsilon)$ for normal (inverted) ordering.

From eq. (21)

$$\tan\theta_{23} = \frac{1 - \frac{\kappa}{\sqrt{2}}\frac{x}{y}\cos\phi_2}{1 + \frac{\kappa}{\sqrt{2}}\frac{x}{y}\cos\phi_2} \quad , \tag{23}$$

Using eqs. (20) and (22),

$$\tan\omega = \frac{2\sin\theta_{13}\cos\delta}{\tan 2\theta_{12}} \ . \tag{24}$$

The corresponding result for real M_R – eq. (16) – is recovered if $\cos\delta = \pm 1$. From eq. (24) θ_{23} is in the first octant if δ lies in the first or the fourth quadrant – which result in opposite signs of J – otherwise it is in the second octant. This correlation does not depend on the mass ordering. Thus the first (second) octant goes with $\delta = 3\pi/2 + \epsilon$ $(3\pi/2 - \epsilon)$ if δ is near $3\pi/2$.

If m_D and m_R are expressed in terms of $\sin\theta_{13}\cos\delta$, one finds

$$\Delta m^2_{solar} = \mathrm{sgn}(\cos\phi_2)\ m^- m_1^{(0)}\ \frac{4\sin\theta_{13}\cos\delta}{\sin 2\theta_{12}} \ , \tag{25}$$

which is of very similar form as eq. (12) for real M_R. Obviously, eqs. (13) and (14) still apply. If one notes the factors which determine the sign of $\cos\delta$ one can conclude that the positivity of Δm^2_{solar} is ensured if $\mathrm{sgn}(\cos\phi_1\cos\phi_2)$ is positive for both mass orderings. Therefore, the sign of the solar mass splitting accommodates both octants of θ_{23} irrespective of the mass ordering. The admissible range of δ can be identified by reexpressing eq. (14) as:

$$|\cos\delta| = \left(\frac{\Delta m^2_{solar}}{|\Delta m^2_{atm}|}\right)\left(\frac{\sin 2\theta_{12}}{4\sin\theta_{13}\ z}\right) \quad . \tag{26}$$

In the analysis which we report m_0, θ_{13}, and θ_{12} are the inputs. We get δ and θ_{23} from eqs. (26) and (24). The CP-violation measure, J, and the combination $|m_{\nu_e\nu_e}|$ which contributes to $0\nu2\beta$ are then easily obtained.

The results for complex M_R are presented in Fig. 2. The left panel (thick curves) shows the variation of θ_{23} with m_0 when the neutrino mass square splittings and the angles θ_{13} and θ_{12} cover their 3σ ranges. The thin curves are for the best-fit values. In this figure the green (pink) curves are always for NO (IO) while solid (dashed) curves are for θ_{23} in the first (second) octant. For IO the thick and thin curves are too close for distinction in this panel. Note that $\theta_{23} = \pi/4$ is not consistent with the

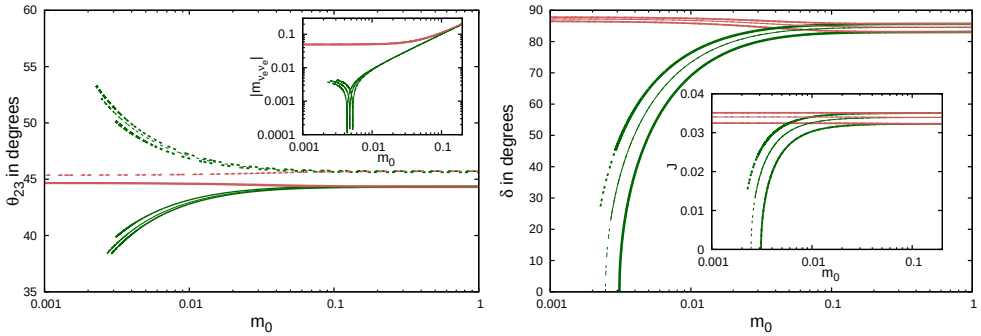

Figure 2: θ_{23}, $|m_{\nu_e\nu_e}|$ (in eV), δ, and J as a function of the lightest neutrino mass m_0 (in eV). The green (pink) curves are for NO (IO). The 3σ allowed region is between the thick curves of each type while the thin curves are for the best-fit input values. The solid (dashed) curves are for the first (second) octant of θ_{23}. Left: The variation of θ_{23}. The inset shows $|m_{\nu_e\nu_e}|$ (in eV), the effective mass controlling $0\nu2\beta$ processes. Right: CP-phase δ. The inset exhibits the CP-violation measure J.

3σ predictions from this model. It is seen that θ_{23} is symmetrically distributed about $\pi/4$, which is expected from eq. (24). For IO the obtained range is outside 1σ but are admissible at 3σ. When θ_{23} is better measured one of the mass orderings will be eliminated unless the neutrinos are in the quasidegenerate regime.

The 3σ limits of θ_{23} in the two octants determine the minimum permitted value of m_0 for NO. For IO eq. (25) allows m_0 to be arbitrarily small (see below). In the inset of this panel $|m_{\nu_e\nu_e}|$ has been plotted. Direct neutrino mass measurements [9] are expected to be sensitive to masses up to 200 meV. Planned $0\nu2\beta$ experiments will access m_0 in the quasidegenerate regime [10]. Fig. 2 indicates that to distinguish the alternate mass ordering possibilities an order of magnitude improvement in their sensitivity will be needed. Large atmospheric neutrino detectors such as INO or long-baseline experiments are alternate avenues for determining the mass ordering.

In the right panel of Fig. 2 the variation of δ with m_0 for both mass orderings is shown. The dependence of J appears in the inset. The two panels of Fig. 2 use the same conventions. Since the three mixing angles are kept in the first quadrant, J is positive if $0 \leq \delta \leq \pi$ and is negative otherwise. As mentioned before, the quadrant of δ can be altered by choosing the quadrant of ϕ_1 suitably[10]. However, for a particular mass ordering from eq. (26) the dependence of $|\cos\delta|$ on m_0 is the same for the different alternatives, which are $\pm\delta$ and $(\pi \pm \delta)$. Keeping this in mind, in Fig. 2 (right panel) δ has been plotted in the first quadrant and J has been taken as positive.

As θ_{23} is symmetric around $\pi/4$ in this model and J is proportional to $\sin 2\theta_{23}$ so it is independent of the octant. For inverted mass ordering both δ and J remain nearly unaffected by variations of m_0.

If m_0 is smaller than 10 meV, then the CP-phase δ is much larger for inverted ordering. Once the mass ordering is known and CP-violation in the neutrino sector is measured this could provide a clear test of this model. Consistent with Sec. III, the limit of real M_R is admissible only for NO, and that too for only a portion of the 3σ range.

As discussed, one has $0 \leq z \leq 1/2$ for NO and $1/2 \leq z \leq 1$ for IO. It is seen from eq. (26) that as

[10]From eq. (22), $\delta \to \pi + \delta$ if $\phi_1 \to \pi + \phi_1$.

a consequence of this the allowed δ are complementary for the two mass orderings tending towards a common value in the quasidegenerate limit, which sets in from around $m_0 = 100$ meV. Unlike the real M_R case, in eq. (14) by taking $\cos\delta$ small one can make $z \equiv m^- m_1^{(0)}/\Delta m^2_{atm} \sim 1$ so that solutions exist for m_0 for IO corresponding to even m_0 arbitrarily small unlike for NO where the lower limit of m_0 is set by $\cos\delta = 1$, i.e., real M_R.

V Conclusions

Summarizing, a neutrino mass model is presented in which the observed solar mass splitting, θ_{12}, θ_{13}, and $\omega = \pi/4 - \theta_{23}$ all originated from a single perturbation (derived out of a Type-I see-saw mechanism) and are thereby related to each other. The atmospheric mass splitting preferred by the data and maximal mixing in this sector play the role of the unperturbed framework. In order to restrict free parameters to a minimum the Dirac term in the see-saw is taken as proportional to the identity matrix and the right-handed neutrino mass matrix, M_R, has a four-zero texture in the flavour basis. Requiring that the mixing angles and solar mass splitting identified by the global fits be reproduced, for a real M_R a narrow range of the lightest neutrino mass ($m_0 \sim$ a few meV) is permitted for normal ordering. It leaves the option open for θ_{23} to belong to the first or the second octant. Such a CP conserving real perturbation forbids inverted ordering. The more general complex M_R enables a considerable enlargement of the range of m_0 and determines in its terms the CP-phase δ and the octant of θ_{23} as well, while accommodating both mass orderings. In the quasi-degenerate limit and in case of inverted ordering $\delta \sim 3\pi/2$ is a natural prediction. Future improved measurements of δ, θ_{23}, $0\nu2\beta$ and determination of the neutrino mass ordering will test the model from various angles.

Acknowledgements

AR thanks the organizers for arranging a very stimulating meeting on neutrino physics. SP acknowledges a Senior Research Fellowship from CSIR, India. AR is partially funded by the Department of Science and Technology Grant No. SR/S2/JCB-14/2009.

References

[1] K. A. Olive *et al.* [Particle Data Group Collaboration], Chin. Phys. C **38**, 090001 (2014).

[2] M. C. Gonzalez-Garcia, M. Maltoni, J. Salvado and T. Schwetz, JHEP **1212**, 123 (2012) [arXiv:1209.3023v3 [hep-ph]], NuFIT 1.3 (2014).

[3] D. V. Forero, M. Tortola and J. W. F. Valle, Phys. Rev. D **86**, 073012 (2012) [arXiv:1205.4018 [hep-ph]].

[4] For the present status of θ_{13} see presentations from Double Chooz, RENO, Daya Bay, MINOS/MINOS+ and T2K at Neutrino 2014. https://indico.fnal.gov/conferenceOtherViews.py?view=standard&confId=8022.

[5] P. Minkowski, Phys. Lett. B **67**, 421 (1977); M. Gell-Mann, P. Ramond and R. Slansky, in *Supergravity*, p. 315, edited by F. van Nieuwenhuizen and D. Freedman, North Holland, Amsterdam, (1979); T. Yanagida, Proc. of the *Workshop on Unified Theory and the Baryon Number of the Universe*, KEK, Japan, (1979); S.L. Glashow, NATO Sci. Ser. B **59**, 687 (1980); R.N. Mohapatra and G. Senjanović, Phys. Rev. D **23**, 165 (1981).

[6] S. Pramanick and A. Raychaudhuri, Phys. Lett. B **746**, 237 (2015) [arXiv:1411.0320 [hep-ph]].

[7] Earlier work on neutrino mass models in which a few elements dominate over others can be traced to F. Vissani, JHEP **9811**, 025 (1998) [hep-ph/9810435]. Models with somewhat similar points of view as those espoused here are E. K. Akhmedov, Phys. Lett. B **467**, 95 (1999) [hep-ph/9909217], and M. Lindner and W. Rodejohann, JHEP **0705**, 089 (2007) [hep-ph/0703171].

[8] For more recent work after the determination of θ_{13} see, for example, B. Brahmachari and A. Raychaudhuri, Phys. Rev. D **86**, 051302 (2012) [arXiv:1204.5619 [hep-ph]]; B. Adhikary, A. Ghosal and P. Roy, Int. J. Mod. Phys. A **28**, 1350118 (2013) arXiv:1210.5328 [hep-ph]; D. Aristizabal Sierra, I. de Medeiros Varzielas and E. Houet, Phys. Rev. D **87**, 093009 (2013) [arXiv:1302.6499 [hep-ph]]; R. Dutta, U. Ch, A. K. Giri and N. Sahu, Int. J. Mod. Phys. A **29**, 1450113 (2014) arXiv:1303.3357 [hep-ph]; L. J. Hall and G. G. Ross, JHEP **1311**, 091 (2013) arXiv:1303.6962 [hep-ph]; T. Araki, PTEP **2013**, 103B02 (2013) arXiv:1305.0248 [hep-ph]; M. -C. Chen, J. Huang, K. T. Mahanthappa and A. M. Wijangco, JHEP **1310**, 112 (2013) [arXiv:1307.7711] [hep-ph]. S. Pramanick and A. Raychaudhuri, Phys. Rev. D **88**, 093009 (2013) [arXiv:1308.1445 [hep-ph]]; B. Brahmachari and P. Roy, JHEP **1502**, 135 (2015) arXiv:1407.5293 [hep-ph].

[9] M. Haag [KATRIN Collaboration], PoS EPS **-HEP2013**, 518 (2013).

[10] W. Rodejohann, Int. J. Mod. Phys. E **20**, 1833 (2011) [arXiv:1106.1334 [hep-ph]].